Journal of Applied Polymer Science

Influence of $BaTiO_3$ Submicrometric Particles on the Structure, Morphology, and Crystallization Behavior of Poly(vinylidene fluoride)

Freddy A. Sánchez, Marta Redondo, Javier González-Benito
Department of Materials Science and Engineering and IQMAAB, Universidad Carlos III de Madrid, 28911, Leganés Spain
Correspondence to: J. González-Benito (E-mail: javid@ing.uc3m.es)

ABSTRACT: Real uniform dispersion of barium titanate, $BaTiO_3$, submicrometric particles within Poly(vinylidene fluoride), PVDF, was achieved to understand induced structure, morphology, and crystallization process of the polymer. Composites with uniform dispersions of $BaTiO_3$ particles within PVDF were accomplished for the first time, blending the polymer with particles by high energy ball milling, HEBM. Different compositions in PVDF/$BaTiO_3$ composite were considered (0, 1, 5, and 10 weight percent of particles). Morphology and structure were studied by scanning electron microscopy, SEM, and X-ray diffraction, XRD, respectively. From dynamic experiments by differential scanning calorimetry, DSC, thermal transitions were determined and melting and crystallization processes were studied. To understand the main mechanism by which specific morphologies can be obtained a deep kinetic analysis of the PVDF crystallization process was carried out. Cooling rate and $BaTiO_3$ content did not provide important variations in the PVDF crystalline structure and morphology; however, the presence of $BaTiO_3$ particles seemed to favor an athermal nucleation, leading to higher fraction of crystals in shorter times. © 2014 Wiley Periodicals, Inc. J. Appl. Polym. Sci. **2015**, *132*, 41497.

KEYWORDS: composites; differential scanning calorimetry; thermoplastics

Received 9 July 2014; accepted 8 September 2014
DOI: 10.1002/app.41497

INTRODUCTION

Addition of little amounts of small particles to a polymer can enhance some of its properties (mechanical, thermal, electrical, optical, etc.) without significant loss in toughness and transparency.[1–3] Nanocomposites based on polymers filled with nanoparticles of electroactive ceramic materials are receiving special attention because they are showing improvements in detection and control, for instance, when they are used as sensors and actuators. Interesting polymers for these systems is poly(vinylidene fluoride), PVDF, and its copolymers because they show opposite piezoelectric response to that of conventional ceramic piezoelectric materials. In particular, playing with the way of poling both phases separately, from having the two phases poled in the same direction to have them poled in opposite directions a gradient of properties are expected.

The most common ferroelectric materials are ceramics, giving the highest electrical responses under a certain mechanical perturbation; however, they are brittle and require high cost processing methods. However, ferroelectric polymers present good mechanical properties, can be processed at relatively low temperature in form of complex shapes, are flexible, and can have relatively high dielectric strengths.[4,5] Hence, the combination of these two kinds of ferroelectric materials (polymer-ceramic composites) seems to be a good way to tune electromechanical properties in materials, keeping the easy processability of the polymer.

PVDF, is a semicrystalline thermoplastic polymer with high thermal and chemical stability; however, its piezoelectric and pyroelectric behaviors usually receive more attention.[6] These properties are highly dependent on its polymorphism (α, β, γ, and δ are its most common crystalline phases). In particular, α-phase arise from the special chains arrangement induced by the trans-gauche conformation (TGTG′). Besides, α-phase has not piezoelectric response since two chains are opposite packed and individual dipole moments are cancelled. In β-phase the chains have all trans conformation (TTTT), resulting in a net dipole moment which yields the highest electroactive properties. γ-phase can be considered intermediate between α and β phases with a gauche bond every fourth repeated units (TTTGTTTG′).[7] α-phase is usually the dominant crystalline form; however, β-phase is the most wanted due to its piezoelectric and pyroelectric properties.[8,9]

However, barium titanate, $BaTiO_3$ is a common dielectric material with very high permittivity and piezoelectric response in its tetragonal structure.[10] Considering that the piezoelectric response in this ceramic material is just the opposite to that of the PVDF, their combination in the form of composites might lead to a gradient of properties by simply playing with the way

of poling both phases separately. However, the final properties of these composites might be greatly affected by morphological and/or structural changes of the polymer induced by the sole presence of the particles. Thus, a deep study of these changes should be done in order to collect the required information to finally understand the macroscopic properties of the composites.

It is well known that uniform particle dispersion is a prerequisite to properly interpret data about the influence of fillers in the properties of a polymer. Due to this, numerous attempts have been made to distribute uniformly particles within a polymer matrix. However, in general, when the ratio between the amount and size of particles is too high, uniform dispersions are rarely achieved. Thermoplastic nancomposites with efficient dispersion of nanoparticles within the polymer matrices were recently prepared with the help of high energy ball milling (HEBM).[11–18] In the case of PVDF based nanocomposites sonication or stirring of suspensions and subsequent casting are probably the most used methods of preparing the final materials.[19,20] However, clear evidences of uniform dispersions are only shown when small content of nanoparticles are used.[21] Besides, the kind of solvent used and evaporation conditions can greatly influence the structure and morphology of the PVDF[22,23] and this might mask the real influence of the particles. Therefore, other methods of nanocomposite preparation should be explored to understand the real influence of the presence of nanofiller on the structure and morphology of the PVDF, avoiding the influence of other variables such us specific interactions with the small molecules of a solvent and conditions of evaporation. Melt blending is another possibility but when preparing PVDF based nanocomposites aggregates of particles were observed.[24]

In this research, a new way of dispersing nanoparticles in PVDF was inspected, HEBM. Besides, the effect of the presence of well dispersed $BaTiO_3$ submicrometer particles on the structure, morphology, and the crystallization process of PVDF was studied. In particular, nonisothermal crystallization and melting experiments of neat PVDF and PVDF/$BaTiO_3$ nanocomposites were performed taking into account two variables: (i) the crystallization rate and (ii) the amount of $BaTiO_3$ particles. Finally, a deep kinetic analysis of the PVDF crystallization process was carried out in order to understand the mechanism by which a specific structure and morphology is obtained.

EXPERIMENTAL

Materials and Sample Preparation

Poly vinylidene fluroride, PVDF ($M_n = 107{,}000$ and $M_w = 275{,}000$), supplied by Sigma-Aldrich was used as the polymer matrix. However, barium titanate, BT, submicrometer particles (99% purity, average diameter 200 nm and density 6.02 g/cm^3) purchased from Nanostructred and Amorphous Materials Inc were used as the filler in the composites.

Composites were prepared as follows: (i) PVDF pellets were grinded using MF 10 Basic Microfine miller. Approximately 15 g of pellets were immersed into liquid nitrogen for 5 min and subsequently grinded at 3000 rpm for 5 min. (ii) Nanocomposites in the form of powder were prepared by mixing the grinded PVDF with BT and subsequent milling by high energy ball milling, HEBM, under cryogenic conditions. Samples of different weight percent compositions (% wt) were prepared: 0, 1, 5, and 10% of BT, respectively. Codes to identify each sample were named as follow: PVDF-XX-BT, where XX represents the weight percent of barium titanate within the PVDF. Mechanical milling was carried out in a MM400 RESTCH apparatus using 15 stainless steel balls of 9 mm of diameter subjecting the mixtures to 1 h of active milling at 25 Hz. Every 5 min of active milling the samples were remained for 15 min under liquid nitrogen to ensure the cryogenic conditions.

Techniques

The dispersion of the barium titanate particles and the morphology of the polymer composites were observed using a scanning electron microscope Phillips XL30. Samples in the form of powder were gold coated by a conventional sputtering method to avoid electrical charge accumulation. Images were obtained from secondary, SE, and backscattered, BSE, electrons signals, respectively. Besides, microanalysis at specific sites were carried out using a DX4i coupled energy dispersive X-ray spectroscopy, EDAX, detector.

Nonisothermal crystallization and melting processes of PVDF were studied by differential scanning calorimetry, DSC, using a Mettler Toledo 822 under a Nitrogen atmosphere (flow rate of 45 mL/min). Samples of about 5 mg were measured. They were first heated up from 25 to 210°C at 100°C/min, maintaining this temperature for 10 min to erase any thermal history. Then, the samples were cooled down to 25°C at different cooling rates (1, 2, 5, 10, and 20°C/min) to study the nonisothermal crystallization process. Finally, a heating scan from 25 to 210°C at 10°C/min was performed to study the melting process of those samples crystallized at different cooling rates. All samples were run at least two times to ensure reproducibility. From cooling and its subsequent heating DSC traces information of crystallization and melting processes was obtained taking into consideration two variables: cooling rate and amount of particles.

X ray diffraction, XRD, was used to identify and analyze the different crystalline phases appearing in the composites. A Philips X'Pert X ray diffractometer with antiscattering diffraction slit of 1°, proportional counter, Ni filter and K_α(Cu) radiation of wavelength, $\lambda = 1.54056$Å was used. Measurements were carried out at 2θ scanning angles from 10° to 50°.

Analytical Considerations

Using the enthalpy of crystallization, ΔH_c, the crystalline fraction or the crystallization degree, X_c, was calculated from the eq. (1):

$$X_c = \frac{\Delta H_c}{\Delta H_m^0 (1-x)} \quad (1)$$

where x is the mass fraction of BT particles and ΔH_m^o is the enthalpy of fusion for the neat PVDF fully or 100% crystallized ($X_c = 1$), $\Delta H_m^o = 104.6$ J/g.[25]

Several analytical methods have been used to describe and study the nonisothermal crystallization kinetics of polymers. Most of them are based on the Avrami equation:[26,27]

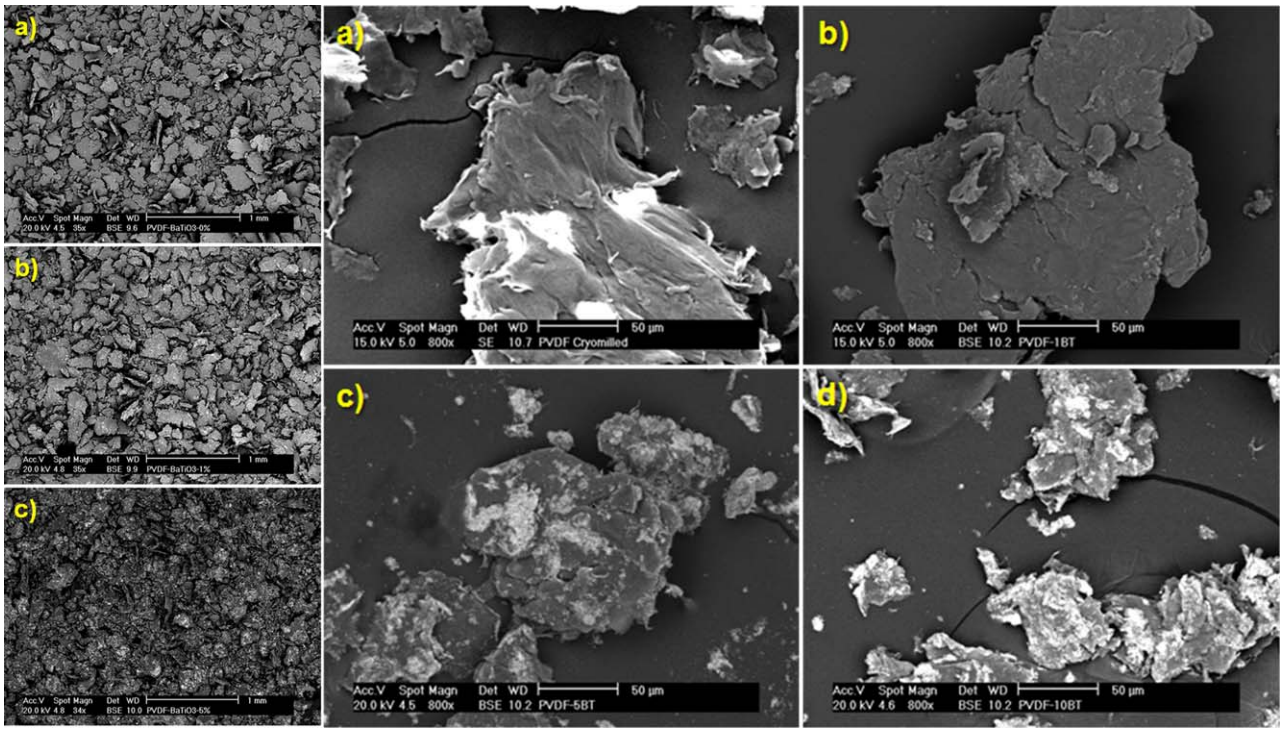

Figure 1. SEM images with low magnification of the milled samples under study: (a) PVDF-0BT; (b) PVDF-1BT; (c) PVDF-5BT; and (d) PVDF-10BT. [Color figure can be viewed in the online issue, which is available at wileyonlinelibrary.com.]

$$X_t = 1 - \exp\left(Z_t \cdot t^n\right) \tag{2}$$

$$ln[-ln(1-X_t)] = n \cdot lnt + lnZ_t \tag{3}$$

where X_t is the degree of crystallinity or the fraction of material crystallized (in terms of weight) at a certain crystallization time, t; n is the Avrami exponent, which depends on the type of crystal nucleation and growth and Z_t is the growth rate constant, which depends on nucleation and crystal growth. However, the Avrami equation was developed for an isothermal crystallization process and in principle, it should not be possible to be used to fit data obtained from nonisothermal experiments. Due to this, several researchers have tried to modify the equation in order to use it and explain the crystallization under conditions close to the manufacture processes or nonisothermal conditions. For instance, Jeziorny[28] modified the eqs. (2) and (3) correcting Z_t by Z_c, considering that the former depends on the cooling rate, Φ, in the following way:

$$lnZ_c = lnZ_t/\Phi \tag{4}$$

However, Ozawa modified the Avrami's equation for a non-isothermal treatment,[29] assuming that the process is formed by infinite number of isothermal steps. According to the Ozawa's theory, the degree of crystallinity can be expressed as

$$X_t = 1 - exp(-K(T)/\Phi^m) \tag{5}$$

where m is the Ozawa's exponent that depends on the dimension of crystal growth, and $K(T)$ is the cooling function.

Combining the equations of Avrami and Ozawa, Liu et al.[30] proposed another formulation to analyze the data obtained from non-isothermal experiments.

$$\text{Ln}\ \Phi = \text{Ln}F(T) - \alpha \text{Ln}t \tag{6}$$

where the parameter $F(T)$ is equal to $[K(T)/Z_t]^{1/m}$ and α is the ratio between the Avrami's exponent, n, and the Ozawa's exponent, m ($\alpha = n/m$). $F(T)$ refers to the value of cooling rate that must be selected within a unit of crystallization time when the systems reach a certain degree of crystallinity. Considering the eq. (6), the plot of ln Φ *vs.* ln t should give a straight line whose zero intercept would be ln $F(T)$ and its slope $-\alpha$.

However, assuming that the crystallization mechanism does not change as it occurs different ways of analyzing the kinetics of the process have been proposed. In general, they are focused to finally obtain the activation energy of the process, E_a (defined as the necessary energy to transport polymer segments to the growing crystal surface). For instance, from the values of the temperature at which the crystallization process is faster, T_p, or the crystallization peak temperature measured by DSC at different cooling rates it is possible to estimate E_a based on the formulation proposed by Kissinger.[31]

$$\frac{d\left[\ln\left(-\frac{\Phi}{T_p^2}\right)\right]}{d\left(\frac{1}{T_p}\right)} = \frac{\text{E}_\text{a}}{R} \tag{7}$$

where R is the general gas constant. In this case, representing ln (Φ/T_p^2) vs. $(1/T_p)$ a straight line should be obtained from whose slope an apparent activation energy, E_a, could be extracted.

RESULTS AND DISCUSSION

Morphology and Dispersion of the $BaTiO_3$ Particles

After cryomilling SEM images with low magnification showed a flake-like morphology for the materials under study (Figure 1).

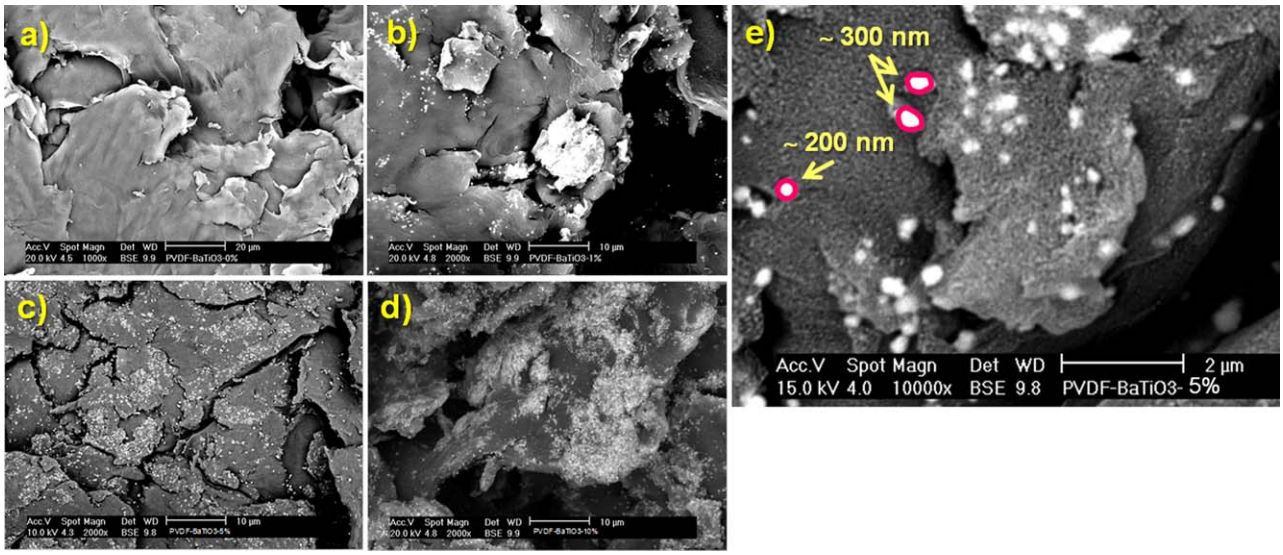

Figure 2. SEM images obtained from BSE of the milled samples under study: (a) PVDF-0BT; (b) PVDF-1BT; (c) PVDF-5BT; (d) PVDF-10BT; and (e) PVDF-5BT at higher magnification. [Color figure can be viewed in the online issue, which is available at wileyonlinelibrary.com.]

In principle, when the milling takes place at the liquid nitrogen temperature, well below the glass transition temperature of the PVDF (−35°C), the polymer should have a brittle behavior. However, clear evidences of plastic deformation are observed, for instance, lines arising from the plastic flow (Figure 1).

However, in the case of composites (Figures 1 and 2) gray matrices with uniformly dispersed bright domains are observed. The average diameter measured for those bright domains was within the range 200–250 nm [see Figure 2(e)]. All these results point out that the bright domains are the BT particles uniformly dispersed in the PVDF polymer represented by the gray matrices. In fact, microanalysis made by X-ray spectroscopy on the bright domains showed a high concentration of Ba and Ti, which is in concordance with the assignation of BT particles to the bright domains.

These results suggest that the particle-polymer blending process took place from the imposition of important shear forces by the hard balls. They allow randomly embedding the BT particles within the PVDF to finally obtain uniform dispersions of them.

In Figure 3, DSC traces showing the crystallization exotherms of the PVDF in the neat PVDF and the PVDF/BT composites are presented. It is clearly observed how the crystallization process is composed by only one exothermic peak. Besides, the higher the cooling rate is the lower the temperature at which the crystallization process is faster, T_p (the peak temperature, Table I). This result shows the kinetic character of the process and the so-called supercooling phenomena. However, a tendency of increasing the crystallization temperature, T_p, the higher the BT particle content is also observed (Table I). It seems that the presence of BT particles favors the crystallization from a nucleation effect that would allow the process to start earlier at higher temperatures.

However, in Figure 4 the melting behavior of the materials under study is shown. It can be seen that the peaks are broader when the preceding cooling processes are faster. Besides, this effect is enhanced with the addition of BT particles. In fact, a new melting contribution at lower temperatures is observed for compositions of 5 and 10%.

Thus, when the preceding cooling is carried out fast enough the PVDF based composites under study show a bimodal melting process for which the contribution at lower temperature increases as the BT content increases (Figure 4). There are mainly three interpretations about the origin of similar multiple melting process in other systems: (i) the existence of different crystalline structures[32,33]; (ii) the appearance of different morphologies[34] and (iii) a fast crystallization might produce small/imperfect crystals that melt and recrystallize during heating to form thicker/less imperfect crystals and then remelt at higher temperatures.

From AFM results D. Olmos et al. shown that the aspect ratio of the PVDF lamellas increases with the amount of BT in cryo-milled samples processed as films.[35] However, XRD experiments did not show any appreciable difference in the relative contribution of the PVDF crystalline phases when either the cooling rate or the BT content is changed (Figure 5). Here, it is interesting to highlight that when $BaTiO_3$ nanoparticles are within the PVDF, apart from its expected diffraction peaks, the typical split of the tetragonal structure is observed at 45° and 45.5° due to the planes (002) and (200), which come from the cubic cell distortion[36] according to the JCPDS chart #5-626. This result is ensuring that the milling process does not alter the $BaTiO_3$ structure retaining therefore its piezoelectric properties.

Therefore two are the most plausible explanation for the multiple melting process observed. The first one considers that higher loaded BT blends that crystallize faster might produce smaller/imperfect crystals that melt–recrystallize during heating to form thicker/less imperfect crystals and then remelt at higher temperatures. The second one is based on Olmos's results,[35] the existence of multiple endotherms can be interpreted considering that spherullites and/or lamellar sizes (morphology) depend on

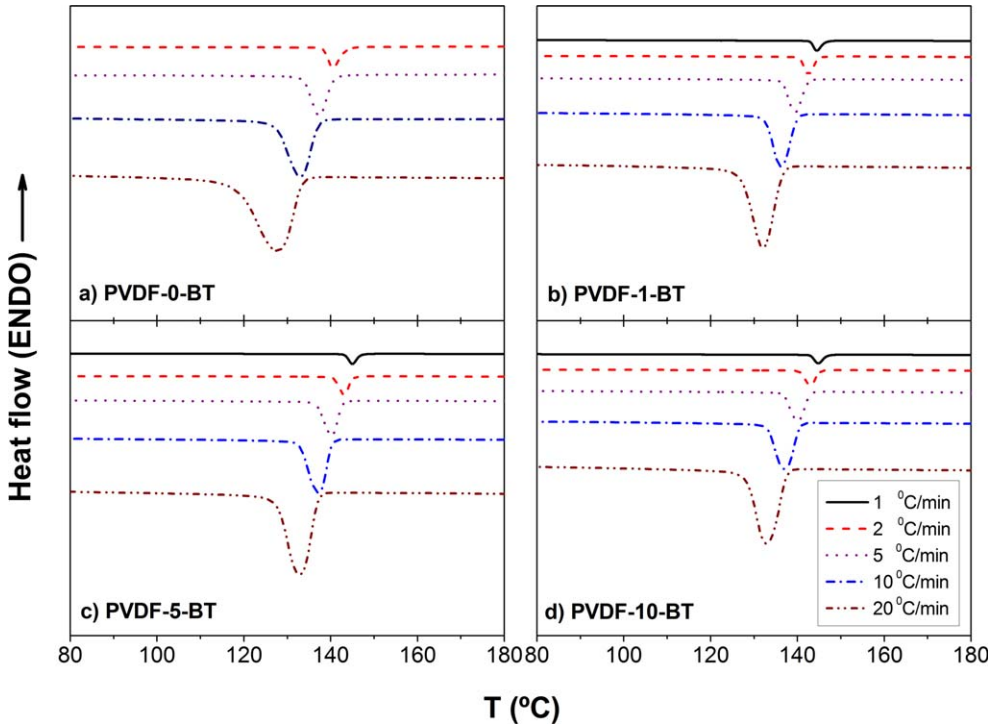

Figure 3. Nonisothermal DSC thermograms for the crystallization of PVDF and PVDF/BT composites at different cooling rates. [Color figure can be viewed in the online issue, which is available at wileyonlinelibrary.com.]

the cooling rate and the presence of BT particles. A slower crystallization process should imply more diffusion time for the macromolecular chains, favoring the growing of crystallites and therefore their homogeneity in terms of size (narrow melting temperatures distribution). However, the addition of BT particles might promote the heterogeneous nucleation and growth, leading to a faster crystallization process with a broader or even multimodal distribution of crystallites sizes what would imply broader distribution of melting temperatures.[20]

Table I. Data Extracted from the Nonisothermal Crystallization Exotherms for all the Samples Under Study at Different Cooling Rates

Sample	Cooling Rate (°C/min)	T_p (°C)	X_c (%)	ΔH_c (J/g)	T_m (°C)
PVDF-0-BT	2	140.7	42	44	170.4
	5	137.3	47	49	169.8
	10	132.8	48	50	169.6
	20	127.0	47	49	170.3
PVDF-1-BT	1	144.5	44	46	167.8
	2	142.5	48	51	167.3
	5	139.7	52	54	167.3
	10	136.2	52	54	166.7
	20	132.0	51	54	166.8
PVDF-5-BT	1	145.5	50	52	167.5
	2	143.2	54	57	166.8
	5	140.2	53	56	166.5
	10	137.2	52	54	165.5
	20	132.7	51	53	164.8
PVDF-10 BT	1	145.0	53	55	166.9
	2	143.3	56	56	166.5
	5	140.4	55	57	166.0
	10	136.8	52	55	165.2
	20	133.0	50	52	164.5

The enthalpy (ΔH_c) and temperature of crystallization (T_p) were obtained from the integration of the exothermic peak and the temperature at the maximum crystallization rate respectively while, the melting points (T_m) were obtained from the peaks of the heating DSC traces. In Table I, all these data are gathered so as the crystallization degree, X_c, for all the samples under study. It is observed that as the cooling rate increases, the T_p value shifts to lower temperatures for both, the neat PVDF and PVDF/BT composites. This result suggests that the lower the cooling rate is, the earlier the crystallization occurs. When semicrystalline polymers are quickly cooled from the melt, it is generally accepted that more supercooling (lower temperature) is required to initiate the crystallization.[30,37] However, regardless the cooling rate, the incorporation of BT particles leads to an increase of T_p (about 4°C) or less supercooling, which suggests a nucleation enhancement.

Besides, it was observed that the crystallinity of PVDF clearly increased with the incorporation of BT (Table I). The maximum increment of X_c was close to 14% for the most loaded PVDF/BT composite (PVDF-10-BT sample) crystallized at 2°C/min. Submicrometric particles may affect the crystallization behavior, participating either in the nucleation and/or the crystal growth stages.[38,39] To have more information about the mechanism of

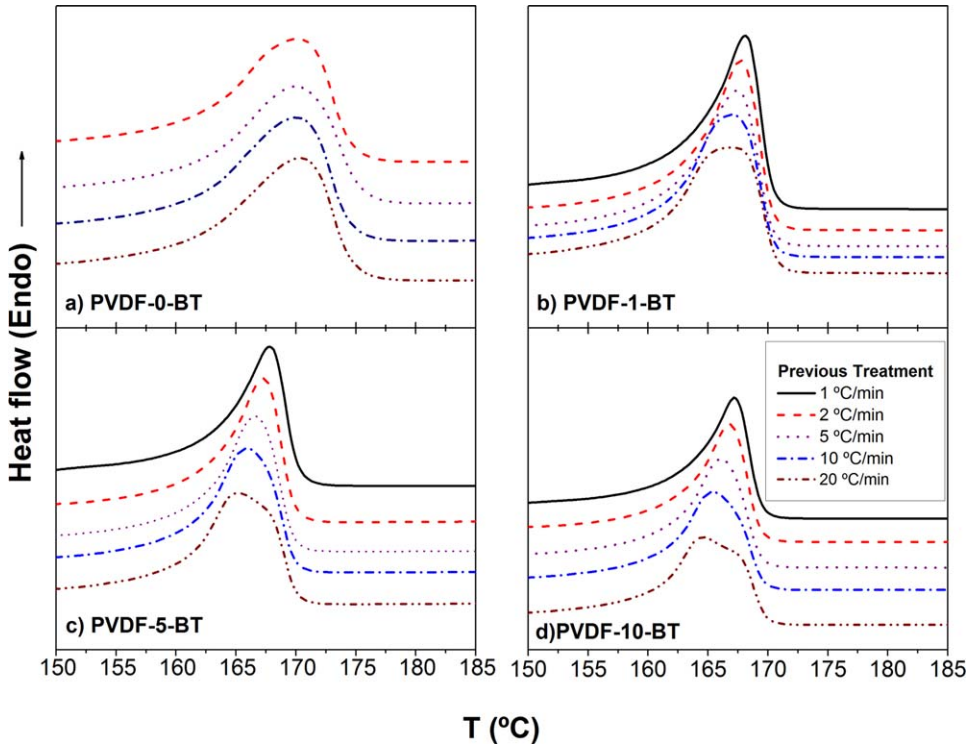

Figure 4. DSC melting curves at 10°C/min for neat PVDF and PVDF/BT nanocomposites after the different nonisothermal crystallization treatments. [Color figure can be viewed in the online issue, which is available at wileyonlinelibrary.com.]

the PVDF crystallization process the evolution of the crystallinity as a function of time should be studied. The relative crystallinity or degree of crystallinity at a certain crystallization time (X_t), was obtained using the following equation[40]:

$$X_t = \frac{\int_{t_0}^{t} H_c dt}{\int_{t_0}^{t_\infty} H_c dt} \quad (8)$$

where t_0 and t_∞ are the onset and end-crystallization times respectively and H_c the enthalpy of crystallization as a function of time. The plot of the degree of crystallinity (X_t) as function of time (t) for the samples under study is shown in Figure 6.

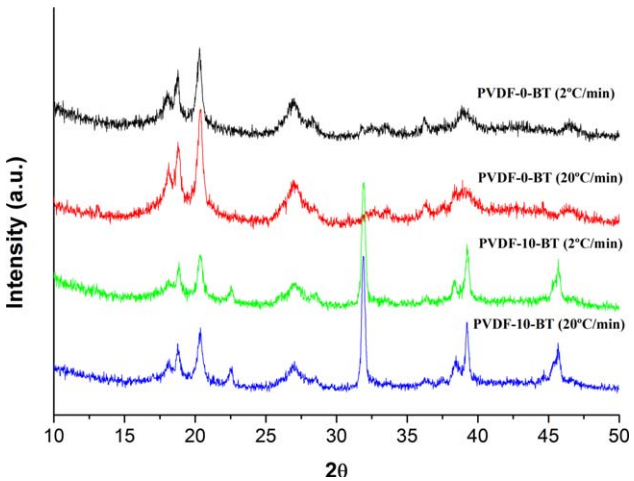

Figure 5. XRD patterns for the films of PVDF and PVDF based composite with 10 wt % of $BaTiO_3$ particles prepared by cooling from the melt at 2 and 20°C/min, respectively. [Color figure can be viewed in the online issue, which is available at wileyonlinelibrary.com.]

Typical sigmoidal profiles were obtained in all cases. Two main observations can be made as a function of cooling rate: (i) the crystallization rate increases and (ii) in general, the crystallization degree at infinite time increases (Table I) although this tendency seems to change when the amount of BT particles increases. The first result is what anyone would expect since the temperatures required for the crystallization were reached faster. The second might be interpreted considering that the mechanism of nucleation is not or poorly dependent on the cooling rate and higher amount of crystals were obtained simply because the process has been faster. However, two main observations can be made when the amount BT is considered: (i) in general, at any cooling rate the final degree of crystallinity increases with the amount of BT particles and (ii) when BT particles are present the final degree of crystallinity starts decreasing at a certain cooling rate value. The first result can be explained from the consideration of a nucleation effect exerted by the presence of BT particles, which favors higher fraction of crystals in shorter times.[41] The second result may be due to the appearance of high number of crystallization nuclei that facilitate a prompt spherulites impingement, leading to more amorphous phase between them (in general, more amorphous phase can be found in the interspherullite regions than in the interlamellar regions).

Kinetics of Crystallization

To take into account nonisothermal conditions, a modified Avrami model was used to analyze the kinetics of the PVDF crystallization as a function of BT particles content. The double logarithm $ln[-ln(1-X_t)]$ versus lnt was represented in Figure 7.

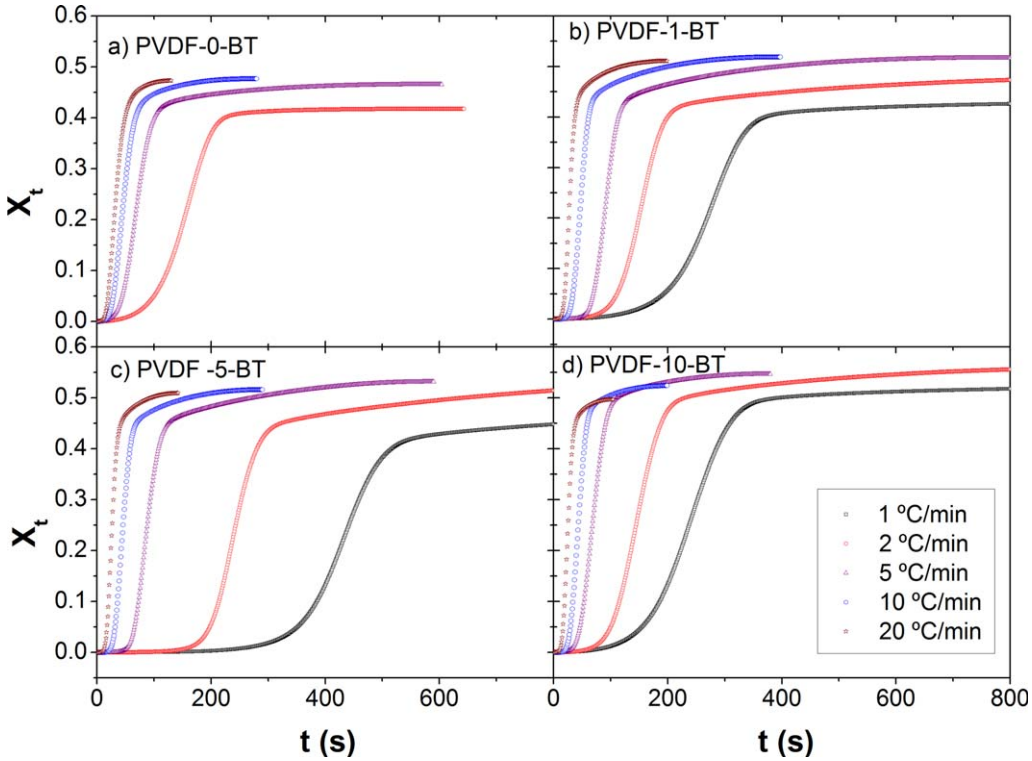

Figure 6. Degree of crystallinity as a function of time for the neat PVDF and PVDF/BT composites at different cooling rates. [Color figure can be viewed in the online issue, which is available at wileyonlinelibrary.com.]

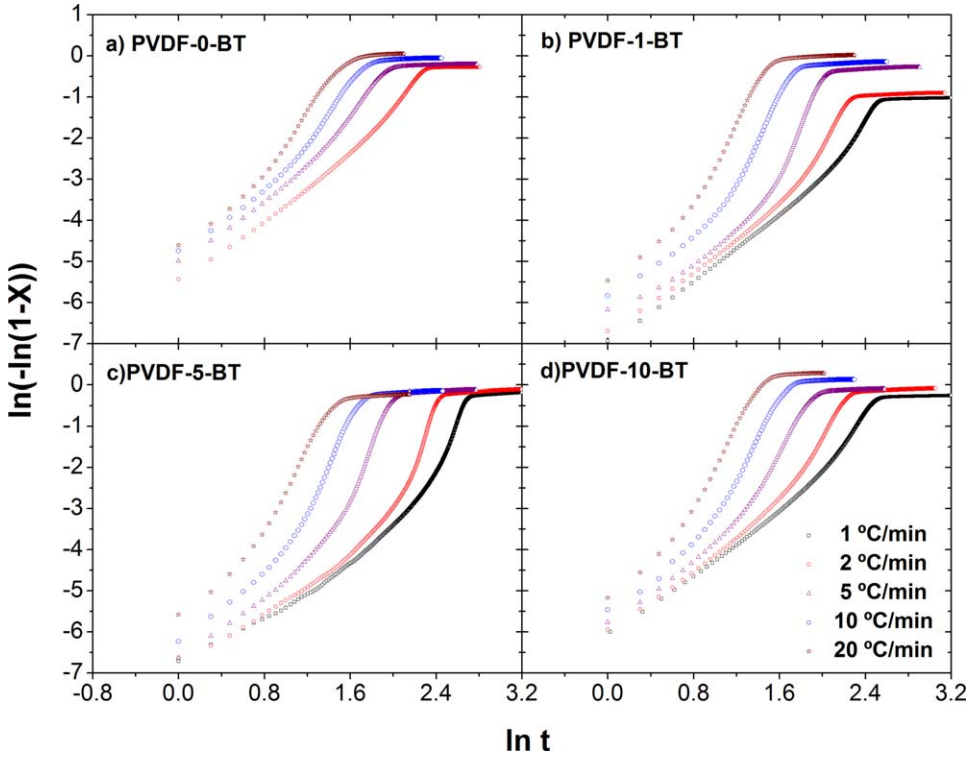

Figure 7. Avrami representations for all the samples under study and at different cooling rates. [Color figure can be viewed in the online issue, which is available at wileyonlinelibrary.com.]

Table II. Nonisothermal Crystallization Kinetic Parameters of Neat PVDF and PVDF/BT Composites Obtained from the Avrami Analysis

Sample	Cooling rate (°C/min)	n_A	$Z_{cA} \times 10^3$	n_B	$Z_{cB} \times 10^3$
PVDF-0-BT	2	2.0	60.3	3.0	24.9
	5	2.2	351	3.6	238
	10	2.1	610	3.9	501
	20	2.5	784	4.3	325
PVDF-1-BT	1	2.0	0.80	2.6	0.30
	2	2.1	30.3	3.1	13.4
	5	2.1	254	4.1	159
	10	2.4	520	4.2	453
	20	2.8	729	4.3	701
PVDF-5-BT	1	1.9	0.70	2.7	0.10
	2	1.7	30.4	3.1	10.5
	5	2.3	231	3.9	162
	10	2.4	521	3.9	455
	20	2.8	745	4.0	714
PVDF-10-BT	1	2.0	1.80	2.9	0.40
	2	2.2	41.4	4.0	9.50
	5	2.3	296	4.0	195
	10	2.8	547	4.0	488
	20	2.8	762	4.1	733

The curves obtained were analyzed considering three different slopes in each linear section observed; therefore, the crystallization process might be represented by three steps: A, B, and C.[14]

From the slopes and intercepts and using eq. (4), the values of the Avrami exponents n and the corrected crystallization rate parameter proposed by Jeziorny,[28] Z_c, were obtained (Table II). The regression coefficients were close to 0.99 in all cases.

Here, it should be taken into account that in nonisothermal crystallization, n might not have the same physical meaning than in isothermal crystallization. It is well known that Avrami

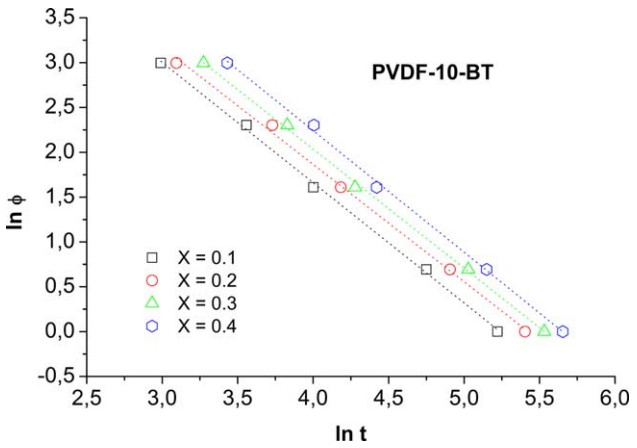

Figure 8. Plots of ln Φ versus ln t for PVDF-10-BT for different degrees of crystallinity (X_t). [Color figure can be viewed in the online issue, which is available at wileyonlinelibrary.com.]

Table III. Nonisothermal Crystallization Kinetic Parameters Based on Liu et al. Treatment[29]

Sample	Parameter	10%	20%	30%	40%
PVDF-0-BT	α	1.4	1.4	1.4	1.5
	$F(T)$	7.1	7.5	8.1	8.5
	r^2	0.969	0.971	0.965	0.970
PVDF-1-BT	α	1.3	1.3	1.3	1.3
	$F(T)$	7.2	7.2	7.3	7.7
	r^2	0.993	0.992	0.994	0.996
PVDF-5-BT	α	1.0	1.0	1.1	1.1
	$F(T)$	5.8	6.2	6.5	6.7
	r^2	0.996	0.990	0.999	0.998
PVDF-10-BT	α	1.3	1.3	1.3	1.4
	$F(T)$	7.0	7.1	7.3	7.7
	r^2	0.998	0.997	0.999	0.999

model does not fit the whole crystallization data since, among other reasons, changes in the crystallization mechanism throughout the whole process may occur. In fact, the appearance of different crystallization regimes (Figure 7) suggests the later. Along region A, the Avrami's exponents, n_A, were fitted to values ranging from 2 to 2.5, which usually is associated to a heterogeneous nucleation process in two dimensions lamellar growth ($n = 2$) or site saturation since it may lead to n values of 1, 2, or 3 for surface, edge and point sites, respectively. Besides, if the distribution of nucleation sites is not random and there is a three dimensional spherulitic growth then, $n = 3$.[42] However, when region B is considered, the values of the Avrami's exponent n_B are between 3 and 4. These values of n are usually associated to a three dimensional heterogeneous ($n = 3$) or homogeneous ($n = 4$) crystal growth. In fact, in this crystallization stage (region B) higher supercooling can be considered inducing therefore athermal or homogeneous nucleation, which is also favored when the cooling rate increases. However, it is always necessary to be very careful with these interpretations since the geometry associated to the crystallization process cannot be clearly inferred from the values of the Avrami's exponent.

Considering now the Z_c values one could say that at a particular cooling rate the overall crystallization rate, Z_c, does not show a clear tendency with the addition of BT particles. However, Z_c increases when the cooling rate increases. These results suggest

Table IV. Apparent Activation Energies E_a for the Nonisothermal Crystallization of PVDF and PVDF/BT Nanocomposites

Sample	Activation Energy (kJ mol^{-1})
PVDF-0-BT	247 ± 33
PVDF-1-BT	342 ± 32
PVDF-5-BT	348 ± 37
PVDF-10-BT	357 ± 35

that the nucleating effect of the BT particles is not substantially affecting the whole crystallization rate.

However, from the use of the eq. (6; Liu et al.[30]) a different approach to describe the non-isothermal crystallization process was also considered. The results are depicted in Figure 8 by plotting ln Φ versus ln t (only results for the PVDF-10-BT sample are shown as an example, the rest of materials gave similar results).

It can be seen a linear relation between both parameters at a given degree of crystallinity. The kinetic parameter $F(T)$ and α values can be obtained from the intercept and the slope respectively (Table III).

Values of $F(T)$ increase with increasing the relative degree of crystallinity indicating that the mechanism of crystallization changes along the process. Besides, $F(T)$ values are lower in the presence BT particles as reported for other particle filled semicrystalline polymers,[43] which indicates that PVDF/BT composites crystallize faster than the neat PVDF.

However, a faster process does not necessary mean energetically favored crystallization. Therefore, the activation energy or, at least, apparent activation energy should be obtained in order to have some additional information about the mechanism of the PVDF crystallization process under the presence of BT particles.

The Kissinger's analytical approach[31] was used to estimate the apparent activation energies, E_a, for the PVDF crystallyzation process in all the samples under study (Table IV). It is observed how the addition of BT particles increases the activation energy of crystallization. Besides, without considering the error, it seems that the higher the BT contents the higher E_a. These results point out that the presence of the BT particles energetically hinders the PVDF crystallization, in other words, the introduction of BT particles leads to a crystallization process controlled by a mechanism with higher activation energy. In principle, the PVDF crystallization process may be explained from the consideration of two contributions nucleation and crystal growth. When crystallization is controlled by homogeneous nucleation, a general mechanism based on the mixture of nucleation and crystal growth is expected since the nucleation is occurring all along the crystallization process. On the contrary, when heterogeneous nucleation is favored, a crystal growth controlled mechanism should be considered. In the later case, in a short period, at the beginning of the crystallization process, the process would be controlled by the nucleation. Although crystal growing is energetically hindered (higher activation energy) this reasoning would indicate that the presence of BT particles must induce faster generation of crystal seeds and consequently faster global crystallization as it was observed.

CONCLUSIONS

A deep calorimetric study of the crystallization and melting process of PVDF, in PVDF/$BaTiO_3$ composites were carried out. The influence of two variables on the PVDF structure and crystallization process was studied: (i) cooling rate and (ii) amount of BT. A slower crystallization showed a narrow melting temperatures distribution that might be explained considering more time of diffusion for the macromolecular chains, favoring the crystallites growing and therefore their homogeneity in terms of size. However, the addition of BT particles might promote the heterogeneous nucleation and growth leading to a faster crystallization process with a wider or even multimodal distribution of crystallites sizes giving broader distribution of melting temperatures. Finally, a mechanism based on nucleation and crystal growth was considered. Under the conditions of crystallization studied, the presence of BT seems to favor an athermal nucleation leading to higher fraction of crystals in shorter times although apparently the global process of crystallization is energetically hindered.

ACKNOWLEDGMENTS

This research has been carried with the funding from the Ministerio de Ciencia e Innovación projects: MAT2010-16815 and AIB2010PT-00267.

REFERENCES

1. Liu, L.; Qi, Z.; Zhu, X. *J. Appl. Polym. Sci.* **1999**, *71*, 1133.
2. Madaleno, L.; Schjodt-Thomsen, J.; Cruz Pinto, J. *Compos. Sci. Technol.* **2010**, *70*, 804.
3. Tang, C. W.; Li, B.; Sun, L.; Lively, B.; Zhong, W. H. *Eur. Polym. J.* **2012**, *48*, 1062.
4. Kulec, J.; Szafraniak, I.; Hilczer, B.; Polomska, M. *J. Non-Cryst. Solids* **2007**, *353*, 4448.
5. Gregorio, R., Jr.; Cestari, M.; Bernardino, F. E. *J. Mater. Sci.* **1996**, *31*, 2925.
6. Eberle, G.; Schmidt, H.; Eisenmenger, W. *IEEE Trans. Dielec. Elec. Insul.* **1996**, *3*, 624.
7. Salimi, A.; Yousefi, A. A. *Polym. Test.* **2003**, *22*, 699.
8. Gregorio, R., Jr.; Capitao, R. C. *J. Mater. Sci.* **2000**, *35*, 299.
9. Sencadas, V.; Gregorio, F. R.; Lanceros-Mendez, S. *J. Non-Cryst. Solids* **2006**, *352*, 2226.
10. Fang, F.; Yang, W.; Zhang, M. Z.; Wang, Z. *Compos. Sci. Technol.* **2009**, *69*, 602.
11. Castrillo, P. D.; Olmos, D.; Amador, D. R.; Gonzalez-Benito, J. *J. Colloid. Interface Sci.* **2007**, *308*, 318.
12. Castrillo, P. D.; Olmos, D.; Gonzalez-Benito, J. *J. Appl. Polym. Sci.* **2009**, *111*, 2062.
13. Gonzalez-Benito, J.; Gonzalez-Gaitano, G. *Macromolecules* **2008**, *41*, 4777.
14. Olmos, D.; Dominguez, C.; Castrillo, P. D.; Gonzalez-Benito, J. *Polymer* **2009**, *50*, 1732.
15. Olmos, D.; Rodríguez-Gutierrez, E.; Gonzalez-Benito, J. *Polym. Compos.* **2012**, *33*, 2009.
16. González-Benito, J.; Castillo, E.; Caldito, J. F. *Eur. Polym. J.* **2013**, *49*, 1747.
17. Olmos, D.; Martínez-Tarifa, J. M.; González-Gaitano, G.; González-Benito, J. *Polym. Test.* **2012**, *31*, 1121.

18. Azhdar, B.; Stenberg, B.; Kari, L. *Polym. Compos.* **2008**, *29*, 252.
19. Yu, K.; Wang, H.; Zhou, Y.; Bai, Y.; Niu, Y. *J. Appl. Phys.* **2013**, *113*, 034105.
20. Mendes, S. F.; Costa, C. M.; Caparros, C.; Sencadas, V.; Lanceros-Méndez, S. *J. Mater. Sci.* **2012**, *47*, 1378.
21. da Silva, A. B.; Arjmand, M.; Sundararaj, U.; Bretas, R. E. S. *Polymer* **2014**, *55*, 226.
22. Gregorio, R., Jr.; Cestari, M. *J. Polym. Sci. Part B: Polym. Phys.* **1994**, *32*, 859.
23. Kwang, M. K.; Jeon, W. S.; Park, N.; Ryu, K. S.; Chang, S. H. *Korean J. Chem. Eng.* **2013**, *20*, 934.
24. Morel, F.; Bounor-Legaré, V.; Espuche, E.; Persyn, O.; Lacroix, M. *Eur. Polym. J.* **2012**, *48*, 919.
25. Marega, C.; Marigo, A. *Eur. Polym. J.* **2003**, *39*, 1713.
26. Avrami, M. *J. Chem. Phys.* **1939**, *7*, 1103.
27. Avrami, M. *J. Chem. Phys.* **1940**, *8*, 212.
28. Jeziorny, A. *Polymer* **1978**, *19*, 1142.
29. Ozawa, T. *Polymer* **1971**, *12*, 150.
30. Liu, T.; Mo, Z.; Wang, S.; Zhang, H. *Polym. Eng. Sci.* **1997**, *37*, 568.
31. Kissinger, H. E. *J. Res. Natl. Bur. Stand.* **1956**, *57*, 217.
32. Andrew, J. S.; Clarke, D. R. *Langmuir* **2008**, *24*, 670.
33. Song, R.; Yang, D.; He, L. H. *J. Matter. Sci.* **2007**, *42*, 8408.
34. Dillon, D. R.; Tenneti, K. K.; Crhistopher, C. Y.; Ko, F. K.; Sics, I.; Hsiao, B. S. *Polymer* **2006**, *47*, 1678.
35. Olmos, D.; Montero, F.; González-Gaitano, G.; González-Benito, J. *Polym. Compos.* **2013**, *12*, 2019.
36. Serra, R.; Gonzalez-Gaitano, G.; González-Benito, J. *Polym. Compos.* **2012**, *33*, 1549.
37. Chen, X.; Wang, L.; Liu, Y.; Shi, J.; Shi, H. *Polym. Eng. Sci.* **2009**, *49*, 2342.
38. Ke, K.; Wen, R.; Wang, Y.; Xie, B. H.; Yang, M. B. *J. Mater. Sci.* **2011**, *46*, 1542.
39. Li, L.; Li, C.; Ni, C.; Rong, L.; Hsiao, B. *Polymer* **2007**, *48*, 3452.
40. Abbasi, S. H.; Hussein, I. A.; Parvez, M. A. *J. Appl. Polym. Sci.* **2011**, *119*, 290.
41. Kim, J. H.; Kwak, S. J.; Man, H. S.; Rock, L. J.; Takahara, A.; Seo, Y. S. *Macromolecules* **2010**, *43*, 10545.
42. Wenzhong, M.; Xiaolin, W.; Zhang, J. *J. Therm. Anal. Calorim.* **2011**, *103*, 319.
43. Lonkar, S. P.; Morlat-Therias, S.; Caperaa, N.; Leroux, F.; Gardette, J. L.; Singh, R. P. *Polymer* **2009**, *50*, 1505.